Simulation of Potentially Catastrophic Landslide Tsunami in North West Borneo Trough

Hock Lye Koh, Wai Kiat Tan, Su Yean Teh, and Mui Fatt Chai

***Abstract*—Seismic–tectonic activity and sedimentary instability processes can generate submarine landslides that seriously damage seafloor infrastructures and generate large destructive tsunamis if the slide volume is high (more than 1 km^3). Sedimentary instability had resulted in a submarine mass failure (SMF) along the North West Borneo Trough (NWBT). This paper presents numerical simulations for a potential landslide tsunami triggered by a SMF in NWBT by a combination of TUNA-LS and TUNA-M2. TUNA-LS simulates landslide tsunami generation based upon an empirical formulation for landslide tsunami initialization. TUNA-M2 solves the 2-D non-linear shallow water equations for simulating tsunami propagation, using tsunami initial conditions calculated by TUNA-LS as input. This landslide tsunami is potentially destructive, with source trough maximum wave height of 120 m. The waves in the front propagate forward in the primary dominant slide direction due northeast. Sabah, Brunei and Sarawak are located in the direction perpendicular to this primary dominant propagation direction. Hence the secondary waves travel southeast towards Sabah, southwest towards Brunei and Sarawak. Simulated offshore wave heights at 50 m depth may reach 15 m to 20 m. Run-up wave heights may exceed 45 m to 60 m depending on locations, exposing communities to extreme hazards.**

***Index Terms*—Brunei slide, landslide tsunami simulation, North West Borneo trough, TUNA.**

I. Introduction

Submarine landslides with mass volume of 1 km^3 or more can potentially generate very destructive tsunamis that can cause extensive damage to seafloor infrastructure. Once in motion, the submarine slide mass can entrain ambient seawater and substrates to form longer and larger runout sediment flows, known as turbidity currents. These turbidity currents can travel hundreds of kilometers and can attain speeds of up to 20 m/s. Submarine landslides, debris flows and associated turbidity currents may pose significant geo-hazards. Research based upon analysis of the most complete compilation of 41 large (1 km^3 or more) submarine landslide in the last 30 thousand years suggests that these hazardous events are temporally random [1], perhaps unrelated to sea level changes [2]. Submarine mass failure (SMF) can generate tsunami with amplitude that far exceeds that generated by co-seismic uplift of seafloor. The initial height of the water displaced by a SMF is highly dependent on the speed at which the mass moves across the sea floor. Fast moving slides are known to produce greater tsunami. The energy of the rapidly sliding mass is transferred to the water at a rate faster than what can be absorbed by the water. Hence, larger volume of water is displaced. Very slow moving slides produce little or no tsunamis. However, where slides move at velocities close or equal to that of the tsunami being generated, they develop in phase, building the waves up to exceptional size.

Tsunamis generated by SMF, or submarine landslides, is a potential major coastal hazards even for moderate earthquakes that occur in or near the coast [3]. Large SMFs are often triggered on the continental slope, as such a landslide's vertical downward displacement may reach several thousand meters. The large potential energy is then transferred to large kinetic energy, generating large tsunamis that leave little time for preparation and or evacuation since the tsunami occurs near the coastal region. For example, in 1946, a magnitude M_W 7.1 earthquake triggered a giant (≈ 200 km^3) submarine landslide along the Aleutian Trench, generating the Unimak, Alaska tsunami [4]. The landslide mass was located within the shallow continental shelf in 150 m water depth, and the landslide mass moved down at a 4° slope to the 4000 m deep Aleutian Trench. Recorded run-up height for this tsunami event reached 35 m above mean sea level at Scotch Cap lighthouse [5].

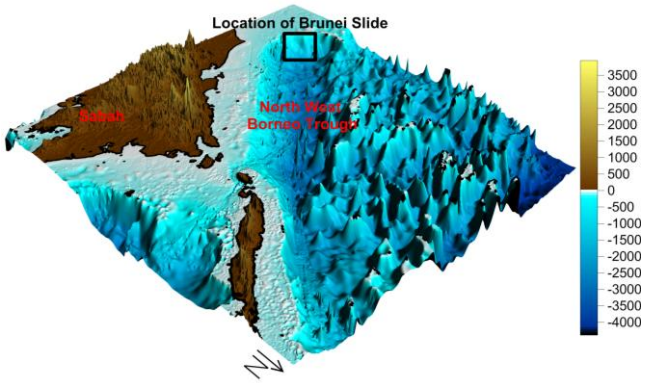

Fig. 1. Location of Brunei slide and the North West Borneo trough.

In this paper, we highlight and assess the tsunami threat along the coast of East Malaysia (Sabah and Sarawak) due to a potential offshore submarine landslide. A past giant landslide seabed debris, known as the Brunei Slide was discovered off the coast of Brunei, suggesting that giant landslide is a recurrent process at that site. The seabed debris

Manuscript received January 9, 2016; revised April 7, 2016. This work was supported by the Ministry of Science, Technology and Innovation under Grant #305/PMATHS/613418.

H. L. Koh is with the Sunway University Business School, Jalan Universiti, Bandar Sunway, 47500 Selangor, Malaysia (e-mail: hocklyek@sunway.edu.my).

W. K. Tan and S. Y. Teh are with the School of Mathematical Sciences, Universiti Sains Malaysia, 11800 USM, Pulau Pinang, Malaysia (e-mail: wk.tan@outlook.com, syteh@usm.my).

M. F. Chai is with the Malaysian Meteorological Department, Jalan Sultan, 46667 Petaling Jaya, Malaysia (e-mail: chai@met.gov.my).

has a volume of 1267 km^3 with an area of 5280 km^2 and a thickness of 240 m. It extends for over 120 km from the Baram Canyon in 200 m water to the deep basin floor of North West Borneo Trough (NWBT), as displayed in Fig. 1. This landslide is an example of a major submarine landslide located on a steep, tectonically active margin adjacent to a large river and canyon system [6].

II. Characteristics and History of Landslide Tsunami

When a mass slides down a slope, the potential energy of the mass is converted to kinetic energy, travelling forward in the direction of the slide. This pushes the water up in the sliding direction. The water being pushed away creates a 'void or vacuum' (negative water level), resulting in the water behind being drawn downward. Therefore, two main waves can be generated during the landslide downward motion onto the seabed. One consists of an elevation wave crest, propagating in the direction of the slide, with speed faster than that of the sliding mass motion. The second wave is a depression wave trough, which is tied to the sliding mass motion, propagating with a slower speed. The sliding mass density and slope steepness are the dominant parameters controlling the dynamics of the slide motion and the associated tsunami waves. The landslide with higher slide density or steeper slope moves faster downslope and generate larger tsunami waves due to the higher kinetic energy. There are two different approaches used for landslide tsunami model formulation regarding the sliding mass characteristics: rigid slide or deformable slide, with significantly different kinematics. For the waves generated by rigid landslide (used in this paper), the wave energy is mostly concentrated on a narrow band of the dominant slide direction. As the rigid landslide continuously accelerates downwards, it can generate very large waves eventually, depending on the slope steepness and distance travelled. This implies that the rigid landslide may create worse scenario for tsunami hazard assessment than that created by deformable landslide. For the waves generated by the deformable landslide, directional spreading is more significant. The waves generated by deformable landslide reach their maximum values earlier than those generated by rigid landslide. At the early stage of the landslide, the deformable landslide achieves higher speed and higher acceleration, resulting in larger surface waves [7].

For the 2011 Tohoku tsunami that killed 20, 000 people, published models of tsunami propagation and coastal run-up under-predict the observed run-up heights measuring up to 40 m along the coast of the Sanriku district in the northeast part of Honshu Island. Grilli *et al*. [8] could not match this largest runup height measured along Sanriku coast between 39.5° and 40.25°N – even using the new co-seismic tsunami sources. Simulations performed by MacInnes *et al*. [9] using ten earthquake sources produced runup heights within 20 % difference from those measured. However, they were unable to match the runup height measured at north of 39°N. The existence of an additional tsunami generation mechanism is suspected to be the cause of this mismatch. While the primary source of the tsunami was the vertical displacement of the seafloor lifted up by the earthquake, an additional tsunami source is also required to account for the unusually high and concentrated waves. The most likely additional tsunami source was a SMF, i.e. a submarine landslide. A slope stability analysis reveals that the horizontal acceleration from the earthquake itself was sufficient large to trigger an SMF. The conclusion that a significant part of the 2011 Tohoku tsunami was generated by an SMF source has important implications for assessment of tsunami hazards in the Tohoku region as well as in other tectonically similar regions. The highly destructive tsunami that devastated the Pacific coast of the Tohoku region located between 35°-43° may strike again. No earthquake-generated tsunami models can satisfactorily reproduce the much elevated tsunami run-ups and extensive inundations measured along the central Sanriku coast. More importantly, inundation distances and run-up elevations along the northern most Sanriku coast are characteristic of an SMF-generated tsunami, because they are more directionally focused than would be expected for an earthquake-only source. Along the central Sanriku coast, the tsunami run-ups and inundations generated by the dual source (earthquake-tsunami plus SMF-tsunami) can reproduce the field observations quite well, whereas the earthquake-seismic source alone severely under-predicts the field observations [10]. This suggests a major, and insufficiently appreciated, tsunami hazard from SMF in this region, as well as in other tectonically similar regions. The need for new approaches to hazard estimation, the uncertainties regarding the past events, and the possibility of SMF-generated secondary tsunamis are challenges that must be addressed in future studies [10].

In a study to assess tsunami hazard in the U.S. East Coast using relationships between submarine landslides and earthquakes, Brink *et al*. [11] concluded that the calculated areas of slope failure at some locations are sufficiently large for earthquakes with magnitude greater than M_w 5.5 to cause a devastating tsunami if the epicenter is optimally located at the base of the upper slope and if the entire area indeed fails. They also suggest that the minimum landslide size that can cause a devastating tsunami can be estimated from tsunami run-up models for selected landslides of different sizes. This information can help in the design of infrastructure facilities to withstand the effects of tsunamis. A successful implementation of this approach may require improvement in the seismic monitoring of continental margins.

The March 13th 1888 lateral collapse of the Ritter Island of Papua New Guinea into the ocean is the largest volcano lateral collapse recorded. The collapse around 6:00 am removed most of the island. This collapse of the volcano was preceded by explosions accompanied by earthquakes. A volume of 4.2 km^3 of mass slided down during the initial collapse, yielding a total volume of 6.4 km^3 in the distal debris flow and turbidity deposits, highlighted the efficiency of substrate erosion during the later stage of the landslide movement under the sea [12]. It produced a large, regionally destructive tsunami that was witnessed by literate observers who timed the waves with watches and provided detailed accounts. That data has been the key to modelling the generation of the tsunami by the landslide and its subsequent propagation [13]. Understanding how submarine landslides from volcano collapses generate these tsunamis is important towards the development of tsunami resilience capability.

The HySEA landslide-tsunami model is used to simulate submarine landslide, tsunami generation, its propagation and the final run-up/inundation of the shoreline in a single coupled model [14]. One of the distinguishing features of the HySEA model is that both the dynamics of the sedimentary fluidized materials and the upper seawater layer are coupled and that each of these two phases influences the other instantly and both are computed simultaneously. The total volume displaced is around 1 km^3 on a slope of 1000 m for the Alboran Sea Basin (SAB) landslide-tsunami. The magnitude of the initial wave at the generation point is significant, reaching about 14 m crust elevation and about 25 m of trough depression for this 1 km^3 slide [14], suggesting the immense destructive capacity of landslide tsunamis.

III. TUNA-LS Simulation Model

There are a variety of landslide tsunami simulation models, with varying levels of mathematical details. Preliminary landslide–tsunami hazard assessment is commonly based on empirical equations derived from wave channel (2D) or wave basin (3D) experiments. The empirical equations developed from "generic" model studies prove to be popular in simulating landslide tsunamis. These generic model studies systematically vary critical parameters such as slide properties, slope angle and length, basin geometry, and water depth [15]. Volume of the mass, initial acceleration, and maximum velocity together determine the characteristics of the initial tsunami generated. In this section, we present a submarine-landslide tsunami generation empirical model, codenamed TUNA-LS, to characterize the initial tsunami at the source of generation triggered by the Brunei Slide. The SMF is modeled as a rigid body moving along a planar slope with center of mass motion $s(t)$ parallel to the planar slope and subject to external forces from added mass, gravity, and dissipation [16], [17]. The SMF geometry is idealized as a mound with elliptical cross-section translating along the planar slope with angle θ from the horizontal, as displayed in Fig. 2. The mound has a maximum thickness T in the center, a total length b along the planar slope axis, a total width w along the cross-section axis, and an initial submergence d at the center. We assume a specific density $\gamma \cong 1.85$, a negligible Coulomb friction coefficient $C_n \cong 0$, an added mass coefficient $C_m \cong 1$, and a drag coefficient $C_d \cong 1$. Then $s(t)$ can be described using (1) [18].

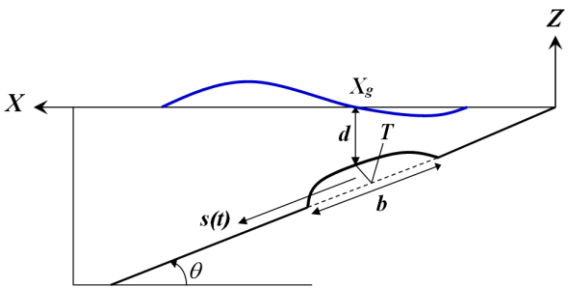

Fig. 2. Schematic figure for underwater slide [18].

$$s(t) = s_0 \ln\left[\cosh(t/t_0)\right] \tag{1a}$$

$$a_0 \cong 0.30 g \sin\theta \tag{1b}$$

$$u_t \cong 1.16\sqrt{bg\sin\theta} \tag{1c}$$

$$s_0 \equiv u_t^2 / a_0 \cong 4.48b \tag{1d}$$

$$t_0 \equiv u_t / a_0 \cong 3.87\sqrt{b/g\sin\theta}. \tag{1e}$$

Here, a_0 is the initial acceleration (m/s^2), u_t is the theoretical terminal velocity (m/s), s_0 denotes a characteristic distance of motion (m), t_0 denotes a characteristics time of motion (s), and g is the gravitational acceleration (m/s^2). Tsunami generation due to SMF has been modeled in two or three dimension using (1), in which these tsunami generation models are based on fully nonlinear potential flow equations solved with a Boundary Element Method (BEM), and have been independently validated both numerically and experimentally [19], [20]. However, such simulations are computationally expensive, particularly in three dimensions. Hence, this complex approach is rarely used in preliminary assessment of landslide tsunami hazards. For preliminary assessment, another popular approach is used to compute all initial tsunami features, such as wavelength λ_0 and amplitude η, as a function of a range of parameter values, and to express the initial features in the form of empirical relationships, as shown in (2) and (3) [21], [22]. These relationships can then be used to predict the tsunami source characteristics. This approach is commonly employed in several tsunami models, such as TUNA-LS (used in this study), GEOWAVE, and COMCOT. The results of TUNA-LS are similar to these models, since they use the same empirical formulations.

$$\lambda_0 = t_0\sqrt{gd}. \tag{2}$$

$$\begin{aligned}\eta \approx{}& 0.723 s_0\left(0.04772 - 0.03559\sin\theta + 0.00813(\sin\theta)^2\right)\\ &\times 1.18(T/B)\left(B\sin\theta/d\right)^{1.25}\left(1-e^{-2.2027(\gamma-1)}\right).\end{aligned} \tag{3}$$

Here, λ_0 is the characteristic wavelength and η is the characteristic wave amplitude. To obtain a two-dimensional tsunami source, the free surface shape of the tsunami waves in the y-direction (direction of slide) can be assumed to be a solitary-like wave form and a double Gaussian function may be used in the x-direction (direction perpendicular to slide) , centered at initial tsunami wave heights at the location (x_0,y_0) [22], as shown in (4).

$$\begin{aligned}\eta_{x,y} = {}& a(-2.25\eta)e^{-\left[-2.52\eta(x-c)/\lambda_0 b\right]^2}\\ &+ be^{-\left[(x-c-\lambda_0/2)/\lambda_0\right]^2}\left(2/\left(e^{3ay/w}+e^{-3ay/w}\right)\right)^2\end{aligned} \tag{4}$$

where

$$a = 1.0 - e^{\left[-2.0906(w/\lambda_0)\right]\left[1+1.09(w/\lambda_0)\right]}$$

$$b = 0.64\eta\left(0.8 + 0.2d/b\sin\theta\right)$$

$$c = 0.95\left[\left(\frac{d+T}{\cos\theta}\right)/\tan\theta + 0.4338 s_0\cos\theta\right] - \left[\left(\frac{d+T}{\cos\theta}\right)/\tan\theta\right]$$

IV. TUNA-LS Simulation Results

In this paper, we consider two scenarios of simulation, with 2° and 4° slopes. Table I summarizes the Brunei Slide parameters for (1) to compute the initial slide motions and initial tsunami characteristics at the source of generation displayed in Table II. The two-dimensional initial tsunamis generated by the Brunei Slide are presented in Fig. 3.

TABLE I: Brunei Slide Parameters

Parameters	2.0° slope	4.0° slope
Length, b (km)	120.0	120.0
Width, w (km)	44.0	44.0
Thickness, T (m)	240.0	240.0
Initial depth, d (m)	2450.0	2450.0

TABLE II: Slide Motions and Initial Tsunami Characteristics

Variables	2.0° slope	4.0° slope
a_0 (m/s^2)	0.102	0.204
u_t (m/s)	234.174	331.070
s_0 (km)	537.212	537.212
t_0 (s)	2294.079	1662.653
λ_0 (km)	355.598	251.522

Based on (1b), a steeper slope angle θ will yield a higher initial acceleration a_0. Therefore, the higher a_0 obtained with a steeper 4° slope is two times that from a milder 2° slope. In addition, based on (1e), a higher a_0 yields a smaller characteristics time of motion t_0, due to the higher velocity of the sliding motion. The steeper 4° slope scenario has a maximum initial velocity of 1.96 m/s, compared to a smaller maximum initial velocity of 0.66 m/s for the scenario with a milder 2° slope. Following (2), λ_0 is proportional to t_0. Thus, the steeper 4° slope scenario yields a wave with a smaller wavelength but with higher amplitude waves than those generated in the milder 2° slope scenario (Fig. 3(c)).

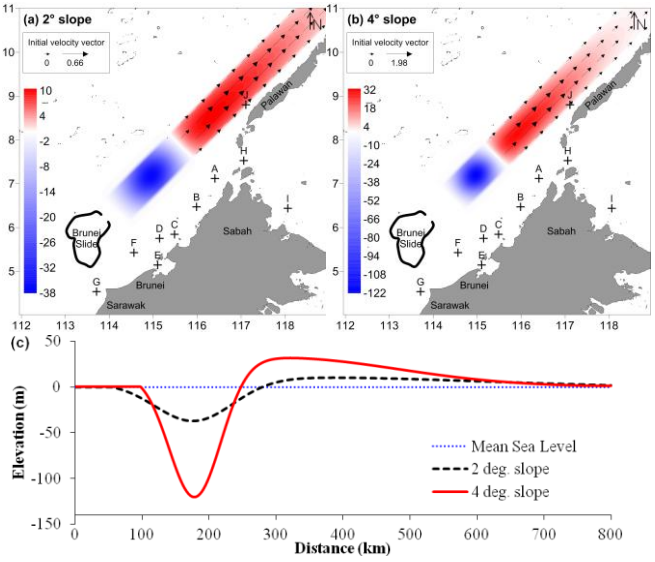

Fig. 3. N-waves tsunamis generated by Brunei Slide: (a) 2.0° slope, (b) 4.0° slope with time series observation points and (c) cross-section view.

The center of Brunei Slide is initially located at latitude of 5.85° and longitude of 113.61° [6]. It then slides downwards to the seafloor in the direction of northeast for a distance of about 211 km. This submarine landslide motion then creates an N-wave, moving in the northeast direction (the direction of slide). The elevation N-wave has a velocity field pointing in the northeast direction, parallel to the sliding direction.

As observed in Fig. 3(c), the wave heights of the N-wave generated by the steeper 4° slope is 3 times those generated by the milder 2° slope. This is because the SMF moves faster in a steeper slope. The higher kinetic energy creates greater energy to push much more water column forward. This results in higher crests and correspondingly deeper troughs. Simulation results by TUNA-LS as illustrated in Fig. 3 are used as the initial source waves for the tsunami propagation simulation model TUNA-M2.

V. TUNA-M2 Simulation Model

The long-wave nonlinear shallow water equation approach is a good approximation for earthquake-generated submarine tsunamis. For landslide-generated tsunamis, this same approach can be used too, producing good results, as demonstrated in the study of the Lituya Bay Mega-Tsunami due to an aerial landslide-generated tsunami [23]. We adopt the same approach in this study. The initial surface water displacement and velocity generated by TUNA-LS are used as input for the model TUNA-M2 to simulate the subsequent propagation of the waves. Wave arrival times and wave heights are recorded during the simulations for assessment and discussion. TUNA-M2 is an in-house tsunami propagation model that employs a finite difference method to solve nonlinear shallow water equations (NSWE), as shown in (5). Details regarding the mathematical formulation and algorithm for TUNA-M2 are available elsewhere [24]-[26].

$$\frac{\partial \eta}{\partial t}+\frac{\partial U}{\partial x}+\frac{\partial V}{\partial y}=0 \tag{5a}$$

$$\frac{\partial U}{\partial t}+\frac{\partial}{\partial x}\left(\frac{U^2}{H}\right)+\frac{\partial}{\partial y}\left(\frac{UV}{H}\right)+gH\frac{\partial \eta}{\partial x}+\frac{gn^2}{H^{7/3}}U\sqrt{U^2+V^2}=0 \tag{5b}$$

$$\frac{\partial V}{\partial t}+\frac{\partial}{\partial x}\left(\frac{UV}{H}\right)+\frac{\partial}{\partial y}\left(\frac{V^2}{H}\right)+gH\frac{\partial \eta}{\partial y}+\frac{gn^2}{H^{7/3}}V\sqrt{U^2+V^2}=0 \tag{5c}$$

Here, η (m) is the water surface displacement measured from mean sea level, d (m) is the water depth, H (m) = η + d is the total water depth, U (m^2/s) and V (m^2/s) are the discharge fluxes in x- and y- directions, g (m/s^2) is the gravitational acceleration, and n (s/m$^{1/3}$) is the Manning friction coefficient.

VI. TUNA-M2 Simulation Results

To set up the simulation, we choose a square computational domain of 756 km × 756 km with a grid size of 900 m in both x- and y- directions with the corresponding computational time step of 1.0 s to ensure numerical stability. Computed tsunami wave heights are then recorded at ten offshore locations situated at 50 m water depth. Fig. 4 displays the TUNA-M2 simulation snapshots at intervals of 10 minutes for the scenario with a 4° slope, while Fig. 5 displays the time

series of wave heights at the ten selected offshore observation points A to J as shown in Fig. 3.

As observed in Fig. 4(a), the initial tsunami waves propagate in two distinct directions. The primary dominant paths of tsunami propagation follow the sliding direction i.e. due northeast. The secondary less dominant waves propagate in the direction perpendicular to the sliding direction, i.e. due southeast and northwest. These secondary less dominant, *leading depression* waves travel towards B, C, D, E, and F located between Sabah and Brunei. On the other hand, the secondary less dominant, *leading-elevation* waves travel towards A, H, and J (A is Kudat, located northwest of the northernmost tip of Sabah; H is Pulau Banggi, located north of the northernmost tip of Sabah; J is Palawan, located at the edge of the dominant leading-elevation wave travelling in the direction of northeast). Hence B, C, D, E, and F receive *leading-depression* waves, while A, H, and J receive *leading-elevation* waves. Since Palawan is closest to the dominant leading-elevation wave than the rest of the ten locations, Palawan (J) has the highest wave height of 22.3 m, followed by Pulau Banggi (H), which receives wave with 19.2 m maximum height.

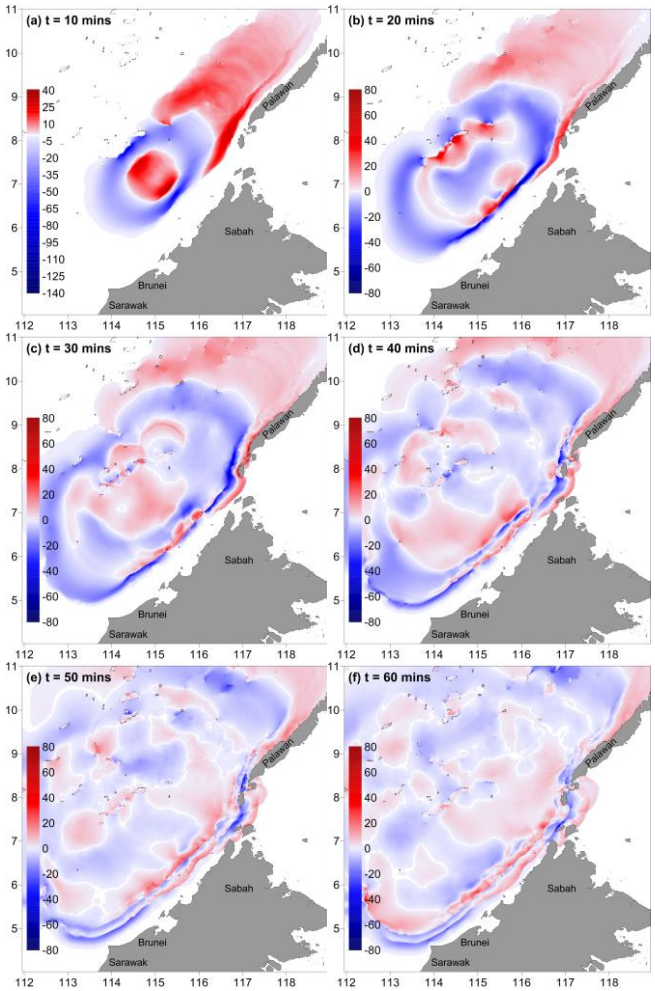

Fig. 4. Tsunami propagation snapshots for 4° slope at intervals of 10 mins, *x*-axis and *y*-axis are presented in longitude and latitude respectively.

We provide a brief observation to provide insights to the data in Fig. 5. The observation point A, located near the northern part of Sabah, is closer to the elevation tsunami source than it is to the depression source. Hence the *leading-elevation* wave, rather than the leading-depression wave, propagates through A first. As observed earlier, observation points B, C, and D (located along the western coast of Sabah north of Brunei) receive a succession of two *leading-depression* N-waves propagating through them. This happens because the second leading-depression N-wave quickly catch up the first leading-depression N-wave as the first enters the shallower water depth region and is hence slowed down.

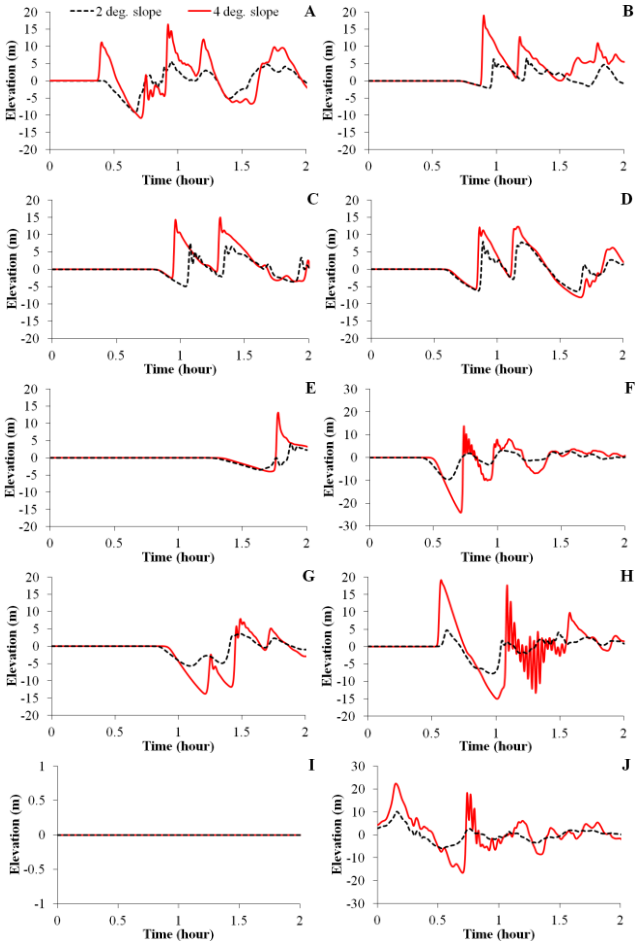

Fig. 5. Time series of simulated wave heights recorded at ten selected observation points A to J for Scenario 1: 2° slope (dashed line) and Scenario 2: 4° slope (solid line).

At t = 10 mins both waves have yet to arrive at any one of the ten observation points. The *first* leading elevation wave begins to arrive at around t = 20 mins at Palawan. At t = 20 mins, the first leading-elevation waves arrive at the dryland of Palawan and continue to propagate towards the islands between southern Palawan and northern Sabah, while the *first* leading-depression waves continue their propagation towards western Sabah, Brunei, and Sarawak. At t = 30 mins, the propagation of the first leading-depression wave is slowed down as it begins to enter shallower water region. At t = 40 mins, the *second* leading-depression waves quickly catch up with the *first* leading-depression waves, closing their distances between them. At t = 50 mins, the first leading-depression waves begin to approach the offshore of Brunei and Sarawak, while the first leading-elevation waves travelling between southern Palawan and northern Sabah have propagated through the islands between them. At t = 60 mins, the first leading elevation waves do not propagate towards eastern Sabah, because the seas between Palawan and Sabah

provide a channel to allow the waves to propagate through in the northeast direction.

Table III summarizes the first leading-elevation wave arrival times and maximum wave heights for observation points A, H, and J. Table IV summarizes the first leading-depression wave arrival times and maximum wave heights for observation points B, C, D, E, F, G, and I. Fig. 6 displays the maximum elevation for the first 2.5 hours of propagation.

TABLE III: ARRIVAL TIME AND MAXIMUM WAVE HEIGHT FOR THE FIRST LEADING-ELEVATION WAVES

Location (Fig. 3)	Scenario 1: 2° slope		Scenario 2: 4° slope	
	Arrival time (hr)	Wave height (m)	Arrival time (hr)	Wave height (m)
A. Kudat	–	–	0.41	11.2
H. Pulau Banggi	0.62	4.7	0.57	19.2
J. Palawan	0.16	10.1	0.16	22.3

TABLE IV: ARRIVAL TIME AND MAXIMUM WAVE HEIGHT FOR THE FIRST LEADING-DEPRESSION WAVE

Location (Fig. 3)	Scenario 1: 2° slope		Scenario 2: 4° slope	
	Arrival time (hr)	Wave height (m)	Arrival time (hr)	Wave height (m)
A. Kudat	0.78	1.6	–	–
B. Penampang	0.98	6.3	0.90	18.9
C. Pulau Tiga	1.08	7.6	0.96	14.2
D. Labuan	0.89	7.9	0.86	12.1
E. Brunei Bay	1.88	4.2	1.78	13.1
F. Seri Begawan	0.78	1.9	0.74	13.7
G. Miri	1.49	3.6	1.49	7.9
I. Sandakan	2.50	0.0	2.50	0.3

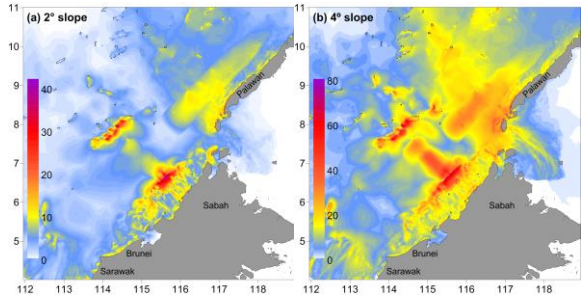

Fig. 6. Maximum elevation for the first 2.5 hours of propagation.

The location of point A deserves additional attention. We have chosen the observation point A to demonstrate an apparent anomaly in the vast difference between the maximum wave height induced by a milder 2° slope as compared to one induced by a higher 4° slope At the observation point A, the simulated peak wave height is 1.6 m for Scenario 1 with a milder 2° slope and 11.2 m for Scenario 2 (which is *7 times* that for Scenario 1) with a steeper 4° slope (*2 times* as steep as a 2°slope). It would have been expected that the peak wave for scenario 2 should be about *2 times* that for scenario 1, instead of *7 times*. This apparent discrepancy is due to the special location of point A (at the border between the elevation source wave and depression source wave), as explained as follows. For Scenario 1, the wave propagating towards the observation point A is a *leading-depression* wave; while for Scenario 2, the propagating wave becomes a *leading-elevation* wave. The stronger motion in Scenario 2 induced by a steeper slope of 4° pushes the tsunami elevation waves further in the northeast direction, thus closer to point A (Fig. 3(b)). The weaker motion in Scenario 1 induced by a milder slope of 2° results in the depression waves closer to point A (Fig. 3(a)). The combination of leading-depression waves created at point A under Scenario 1 is characterized by a drawdown of water followed by an advancing positive wave. The secondary leading elevation wave arriving at the observation point A for Scenario 2 is created by the primary dominant leading elevation waves propagating in the northeast direction, generated by the landslide. From Fig. 3(a) for Scenario 1, it can be seen that the observation point A is located at the border in between the initial positive and initial negative waves generated by the sliding of the mass. This results in a weaker tsunami waves as the opposing positive-negative wave forms tend to neutralize each other. From Fig. 3(b) for Scenario 2, the observation point A is located closer to the primary dominant elevation wave, and hence receives higher tsunami wave heights.

VII. DISCUSSION

This study has simulated the generation and propagation of a potentially giant submarine landslide tsunami in the NWBT. Numerical simulations by TUNA-LS coupled with TUNA-M2 show that the maximum off shore wave heights may reach 20 m for Western Sabah with estimated arrival time of about one hour. Meanwhile, off shore of northeast Sarawak and Brunei may receive maximum tsunami heights up to 15 m, within one and a half hours. Previous run-up simulations performed for Penang and Langkawi indicate that the run-up heights have an amplification factor of 3 or more over the offshore heights [26], [27]. This implies that run-up wave heights along the affected beaches may reach or exceed 45 m to 60 m. A general observation based upon past tsunami events worldwide indicate that run-up heights exceeding the threshold level of 3 m can post severe danger to properties and human lives. Given that the arrival time is short (one to one and a half hour), and given a potential run-up wave heights of the order of 45 m to 60 m (15 to 20 times of 3 m threshold level), the local coastal communities are indeed potentially exposed to high risks should this landslide tsunami occur. This level of extreme risks is indeed unthinkable and unacceptable. Much work needs to be performed towards developing an effective tsunami hazard mitigation program for Sabah (and Sarawak) in order to reduce the exposure. This is a challenging task.

REFERENCES

[1] E. L. Pope, P. J. Talling, M. Urlaub, J. E. Hunt, M. A. Clare, and P. Challenor, "Are large submarine landslides temporally random or do uncertainties in available age constraints make it impossible to tell?" *Marine Geology*, vol. 369, pp. 19-33, 2015.

[2] M. Urlaub, P. J. Talling, and D. G. Masson, "Timing and frequency of large submarine landslides: Implications for understanding triggers and future geohazard," *Quaternary Science Reviews*, vol. 72, pp. 63-82, 2013.

[3] D. R. Tappin, P. Watts, G. M. McMurtry, Y. Lafoy, and T. Masumoto, "The Sissano, Papua New Guinea tsunami of July 1998 — Offshore evidence on the source mechanism," *Marine Geology*, vol. 175, pp. 1-23, 2001.

[4] G. J. Fryer, P. Watts, and L. F. Pratson, "Source of the great tsunami of 1 April 1946: A landslide in the upper Aleutian forearc," *Marine Geology*, vol. 203, pp. 201-218, 2004.

[5] J. F. Lander, *Tsunami Affecting Alaska 1737-1996*, Publication 31, Nat. Geophysical Data Ctr., Nat. Envir. Satellite, Data, and Info. Service, Nat. Oceanic and Atmospheric Admin., U.S., Dept. of Commerce, Boulder, CO, 1996, p. 205.
[6] M. J. R. Gee, H. S. Uy, J. Warren, C. K. Morley, and J. J. Lambiase, "The Brunei slide: A giant submarine landslide on the North West Borneo Margin revealed by 3D Seismic data," *Marine Geology*, vol. 246, pp. 9-23, 2007.
[7] G. Ma, J. T. Kirby, and F. Shi, "Numerical simulation of tsunami waves generated by deformable submarine landslides," *Ocean Modeling*, vol. 69, pp. 146-165, 2013.
[8] S. T. Grilli, J. C. Harris, T. S. Tajalli Bakhsh, T. L. Masterlark, C. Kyriakopoulos, J. T. Kirby, and F. Shi, "Numerical simulation of the 2011 Tohoku tsunami based on a new transient FEM co-seismic source: comparison to far- and near-field observations," *Pure and Applied Geophysics*, vol. 170, pp. 1333–1359, 2013.
[9] B. T. MacInnes, A. R. Gusman, R. J. LeVeque, Y. Tanioka, "Comparison of earthquake source models for the 2011 Tohoku event using tsunami simulations and near-field observations," *Bulletin of the Seismological Society of America*, vol. 103, pp. 1256–1274, 2013.
[10] D. R. Tappin, S. T. Grilli, J. C. Harris, R. J. Geller, T. Masterlark, J. T. Kirby, F. Shi, G. Ma, K. K. S. Thingbaijam, and P. Martin Mai, "Did a submarine landslide contribute to the 2011 Tohoku tsunami?" *Marine Geology*, vol. 357, pp. 344-361, 2014.
[11] U. S. Brink, H. J. Lee, E. L. Geist, and D. Twichell, "Assessment of tsunami hazard to the U.S. East Coast using relationships between submarine landslides and earthquakes," *Marine Geology*, vol. 264, pp. 65-73, 2009.
[12] S. Day, P. Llanes, E. Silver, G. Hoffmann, S. Ward, and N. Driscoll, "Submarine landslide deposits of the historical lateral collapse of Ritter Island, Papua New Island," *Marine and Petroleum Geology*, vol. 67, pp. 419-438, 2015.
[13] S. N. Ward and S. J. Day, "Ritter Island volcano lateral collapse and tsunami of 1888," *Geophysical Journal International*, vol. 154, pp. 891-902, 2003.
[14] J. Macías, J. T. Vázquez, L. M. Fernández-Salas, J. M. González-Vida, P. Bárcenas, M. J. Castro, V. Díaz-del-Río, and B. Alonso, "The Al-Borani submarine landslide and associated tsunami: A modeling approach," *Marine Geology*, vol. 361, pp. 79-95, 2015.
[15] V. Heller and J. Spinneken, "On the effect of the water body geometry on landslide-tsunamis: Physical insight from laboratory tests and 2D to 3D wave parameter transformation," *Coastal Engineering*, vol. 104, pp. 113-134, 2015.
[16] P. Watts, "Water waves generated by underwater landslides," Ph.D. thesis, California Institute of Technology, Pasadena, CA, 1997.
[17] P. Watts, "Wavemaker curves for tsunami generated by underwater landslides," *Journal of Waterway, Port, Coastal, and Ocean Engineering*, vol. 124, pp. 127-137, 1998.
[18] P. Watts, S. T. Grilli, J. T. Kirby, G. J. Fryer, and D. R. Tappin, "Landslide tsunami case studies using a Boussinesq model and a fully nonlinear tsunami generation model," *Natural Hazards and Earth System Sciences*, vol. 3, pp. 391-402, 2003.
[19] S. T. Grilli and P. Watts, "Modeling of waves generated by a moving submerged body. Applications to underwater landslides," *Engineering Analysis with Boundary Elements*, vol. 23, pp. 645-656, 1999.
[20] S. T. Grilli, S. Vogelmann, and P. Watts, "Development of a 3D numerical wave tank for modeling tsunami generation by underwater landslides," *Engineering Analysis with Boundary Elements*, vol. 26, pp. 301-313, 2002.
[21] S. T. Grilli and P. Watts, "Tsunami generation by submarine mass failure. Part I: Modeling, experimental validation and sensitivity analysis," *Journal of Waterway, Port, Coastal, and Ocean Engineering*, vol. 131, pp. 283-297, 2005.
[22] P. Watts, S. T. Grilli, D. R. Tappin, and G. J. Fryer, "Tsunami generation by submarine mass failure. Part II: Predictive equations and case studies," *Journal of Waterway, Port, Coastal, and Ocean Engineering*, vol. 131, pp. 298-310, 2005.
[23] J. M. González-Vida, J. Macías, M. J. Castro, C. Sánchez-Linares, and M. de la Asunción, "The Lituya Bay landslide-generated mega-tsunami. Numerical simulation and sensitivity analysis," *Geophysical Journal International*.
[24] H. L. Koh, S. Y. Teh, P. L. -F. Liu, A. M. I. Izani, and H. L. Lee, "Simulation of Andaman 2004 tsunami for assessing impact on Malaysia," *Journal of Asian Earth Sciences*, vol. 36, pp. 74-83, 2009.
[25] S. Y. Teh, H. L. Koh, P. L. -F. Liu, A. M. I. Izani, and H. L. Lee, "Analytical and numerical simulation of tsunami mitigation by mangroves in Penang, Malaysia," *Journal of Asian Earth Sciences*, vol. 36, pp. 38-46, 2009.
[26] W. K. Tan, S. Y. Teh, and H. L. Koh, "Development of tsunami inundation map for Penang using TUNA-RP," presented at the Simposium Kebangsaan Sains Matematik 23, Johor Bahru, Malaysia, November 24-26, 2015.
[27] H. L. Koh, S. Y. Teh, K. X. Lee, C. K. Ho, and W. K. Tan, "Assessing potential impact of Tsunami on Penang Island via TUNA-RP simulation," presented at the Simposium Kebangsaan Sains Matematik 23, Johor Bahru, Malaysia, November 24-26, 2015.

H. L. Koh was born on May 30, 1948 in Penang, Malaysia. He received his BSc from University of Malaya in 1970 and the MA as well as the PhD in mathematics in 1971 and 1976 respectively from University of Wisconsin, Madison, USA.

He was the recipient of Oppenheim Prize of University of Malaysia and Fulbright Scholarship USA and DAAD Fellowship. He served as an associate member of the International Centre for Theoretical Physics (ICTP) from 1986 to 1992. He is currently a professor at Sunway University Business School. He has served for 40 years in Universiti Sains Malaysia before continuing his research at Sunway University. His fields of specialization include environmental and ecological system modeling and simulations, integrated river basin management and modeling, numerical modeling of tsunami hazards and numerical simulation of dengue and H1N1 epidemics.

Prof. Koh has many journal publications, notably in Water Sciences & Technology, Environmental Monitoring and Assessment, Water Quality Research Journal of Canada, Pollution in the Urban Environment, Journal of Asian Earth Sciences, Ecosystems, Ecological Modelling, Landscape Ecology and Agricultural and Forest Meteorology.

W. K. Tan was born on Nov 11, 1988 in Pahang, Malaysia. He received his BSc as well as MSc in mathematics in 2011 and 2013 respectively from University Sains Malaysia.

In 2014 and 2015, he was sponsored by the International Centre for Theoretical Physics (ICTP) to attend two high performance computing workshops in Trieste, Italy. He is currently a PhD student at School of Mathematical Sciences, Universiti Sains Malaysia, where he also serves as a tutor for C++ programming since 2013. His research interests include tsunami modeling and high performance computing. Mr. Tan has numerous publications in ISI and Scopus proceedings.

S. Y. Teh was born on November 5, 1981 in Kedah, Malaysia. She received her BSc, MSc and PhD in mathematical modeling in 2004, 2005 and 2008 respectively, all from Universiti Sains Malaysia.

In 2006, she was awarded the UNESCO/Keizo Obuchi Research Fellowship to undertake research on "Management Modeling of Everglades Wetlands Hydrology and Ecosystems" at University of Miami. Since then, she has been invited to University of Miami and Nanjing Forestry University under USGS grants and to four workshops at Abdus Salam International Centre for Theoretical Physics (ICTP) at Trieste, Italy under the sponsorship of ICTP. She is currently an Associate Professor at School of Mathematical Sciences, Universiti Sains Malaysia. She works on various topics in ecosystem and environmental modeling, many of which were initiated and driven by the needs of the country or industry. Her research interests revolve around mathematical modeling with particular focus on computational simulation of real-life problems to provide insights and to suggest possible solutions.

Dr. Teh has many articles published in Journal of Asian Earth Sciences, Ecosystems, Ecological Modelling, Landscape Ecology and Agricultural and Forest Meteorology.

M. F. Chai was born on Dec. 08, 1977 in Sabah, Malaysia. He received his BSc in physics in 2001 from Universiti Sains Malaysia and the MSc in disaster management from National Graduate Institute for Policy Studies, Japan in 2008.

In 2011, he was sponsored by the Malaysian Public Service Department under the Federal Training Award Scheme for pursuing a PhD studies on earthquake engineering at Universiti Sains Malaysia. He received his PhD in 2015. His research areas of interests include mathematical modeling of tsunami in submarine landslide and run-up.